THE JOURNAL OF BIOLOGICAL CHEMISTRY
Vol. 272, No. 33, Issue of August 15, pp. 20531–20537, 1997

Printed in U.S.A.

Trimeresurus stejnegeri Snake Venom Plasminogen Activator

SITE-DIRECTED MUTAGENESIS AND MOLECULAR MODELING*

(Received for publication, June 25, 1996, and in revised form, April 11, 1997)

Yun Zhang‡§¶, Anne Wisner‡, Rachid C. Maroun‡, Valérie Choumet‡, Yuliang Xiong§, and Cassian Bon‡‖

From the ‡Unité des Venins, Institut Pasteur, 25 rue du Docteur Roux, 75724 Paris Cedex 15, France and §Kunming Institute of Zoology, Chinese Academy of Sciences, Kunming 650223, Yunnan, China

The specific plasminogen activator from *Trimeresurus stejnegeri* venom (TSV-PA) is a serine proteinase presenting 23% sequence identity with the proteinase domain of tissue type plasminogen activator, and 63% with batroxobin, a fibrinogen clotting enzyme from *Bothrops atrox* venom that does not activate plasminogen. TSV-PA contains six disulfide bonds and has been successfully overexpressed in *Escherichia coli* (Zhang, Y., Wisner, A., Xiong, Y. L., and Bon, C. (1995) *J. Biol. Chem.* 270, 10246–10255).

To identify the functional domains of TSV-PA, we focused on three short peptide fragments of TSV-PA showing important sequence differences with batroxobin and other venom serine proteinases. Molecular modeling shows that these sequences are located in surface loop regions, one of which is next to the catalytic site. When these sequences were replaced in TSV-PA by the equivalent batroxobin residues none generated either fibrinogen-clotting or direct fibrinogenolytic activity. Two of the replacements had little effect in general and are not critical to the specificity of TSV-PA for plasminogen. Nevertheless, the third replacement, produced by the conversion of the sequence DDE 96a-98 to NVI, significantly increased the K_m for some tripeptide chromogenic substrates and resulted in undetectable plasminogen activation, indicating the key role that the sequence plays in substrate recognition by the enzyme.

The plasminogen activator from *Trimeresurus stejnegeri* venom (TSV-PA)[1] is a 234-residue single chain glycoprotein with an apparent molecular weight of 33 kDa (1). Like physiological tissue type plasminogen activator (t-PA), TSV-PA specifically cleaves the Arg^{561}-Val^{562} plasminogen bond to generate two-chain plasmin, a key enzyme in fibrinolysis (2, 3). Sequence homology with trypsin and other venom serine proteinases (4) indicates that TSV-PA belongs to the family of serine proteinases (5). Trypsin-like serine proteinases, which cleave the peptide bond following arginine or lysine, display very different substrate and inhibitor specificities. They were among the first enzymes to be studied extensively (6). In particular, the role of the "specificity pocket" in determining the "primary", or P1,[2] specificity of the enzyme has long been recognized (7). The existence and critical importance of other additional structural determinants of proteinase specificity have also been established (8), but both their location and their role remain unknown.

The sequence of TSV-PA exhibits a high degree of identity (60–66%) with other snake venom proteinases, such as *Vipera russelli* venom factor V activator (9), batroxobin from *Bothrops atrox* venom (10), and *Agkistrodon contortrix* venom protein C activator (11), which present considerable differences in their substrate specificities. For example, TSV-PA, which efficiently activates plasminogen, does not clot or degrade fibrinogen and does not activate or degrade factor X, prothrombin, and protein C (1). On the other hand, batroxobin, which shows a thrombin-like activity (12), does not act on plasminogen. TSV-PA shares a weak sequence identity with the serine proteinase domain of human t-PA (23%) and urokinase type plasminogen activator (u-PA) (21%) yet is functionally analogous to them. Moreover, in common with the highly nonspecific trypsin, TSV-PA is a one-chain enzyme, and it possesses six disulfide bonds, of which five are topologically equivalent; the sequence identity with trypsin is 40%.

For the expression and refolding of recombinant TSV-PA (rTSV-PA) in bacteria we used a strategy similar to the one reported by Maeda *et al.* (13) for batroxobin. This led us to undertake structure-function studies on the substrate specificity of TSV-PA by site-directed mutagenesis to examine the role of particular residue(s) or region(s). We thus looked at three peptide fragments (residues SNNFQ 60–64, DDE 96a-98, and SWRQV 173–176) that show quite different amino acid sequences between TSV-PA and batroxobin. These fragments are located in solvent-exposed loops in a sequence homology trypsin-based three-dimensional model of TSV-PA. Consequently, we exchanged the TSV-PA sequence by the equivalent batroxobin residues by site-directed mutagenesis. A TSV-PA variant whose modifications are located close to the catalytic site lost its plasminogen activation properties.

EXPERIMENTAL PROCEDURES

Materials—Human thrombin, human Lys-plasminogen, and urokinase (two-chain form, M_r 33,000) were obtained from Sigma. Bovine factor Xa was from Pierce. Human fibrinogen (grade L) from Kabi Vitrum was pretreated with diisopropyl fluorophosphate according to the instructions of the manufacturer. Natural TSV-PA was purified from *T. stejnegeri* venom as described before (1). The concentration of

* The costs of publication of this article were defrayed in part by the payment of page charges. This article must therefore be hereby marked "*advertisement*" in accordance with 18 U.S.C. Section 1734 solely to indicate this fact.

¶ Recipient of fellowships from the Fondation pour la Recherche Médicale and from the Sanofi Thrombosis Association during his stay at the Pasteur Institute.

‖ To whom correspondence should be addressed. Tel.: 33 1 45 68 86 85; Fax: 33 1 40 61 30 57; E-mail: cbon@pasteur.fr.

[1] The abbreviations used are: TSV-PA, *T. stejnegeri* venom plasminogen activator; rTSV-PA, recombinant TSV-PA; t-PA, tissue type plasminogen activator; u-PA, urokinase plasminogen activator; PAGE, polyacrylamide gel electrophoresis; Lys-plasminogen, plasmin-derived Lys^{78} plasminogen; SCR, structurally conserved region.

[2] The residues on the acyl group side of the scissile bond, *i.e.* toward the N terminus of substrates, are numbered P1, P2, P3, etc. Those on the C terminus side are denoted P1′, P2′, P3′, etc. The corresponding binding sites on the enzyme for these residues are denoted S1, S2, S3, . . ., S1′, S2′, S3′, etc.

plasminogen was determined by measuring the absorption at 280 nm, using an absorption coefficient $\epsilon_{1\%}$ of 16.8 (14).

Methods

Construction of a TSV-PA Expression Plasmid—The pET expression vector (Novagen) was used for expression of TSV-PA in *Escherichia coli*. To subclone the TSV-PA open reading frame from the cDNA clone D16 into the pET17b vector, a polymerase chain reaction was conducted with a forward primer, En, and a reverse primer, EcR, in the presence of an adapter primer, E. Primer E contains the following elements: 1) a *Bam*HI site to facilitate subcloning (italicized); 2) the coding sequence for a tetrapeptide recognition site of factor Xa (boldface); and 3) 5 N-terminal residues of the TSV-PA coding sequence (underlined): 5′-CC*GGATCC*A**ATCGAAGGTCGT**GTCTTTGGAGGTGAT-3′. Primer En corresponds to the first 24 nucleotides of primer E. Primer EcR, 5′-A*GAATTC***TCA**CGGAGGGCAGGTCGC-3′ is an antisense oligonucleotide that contains the following: 1) an *Eco*RI site to facilitate subcloning (italicized); 2) a stop codon (boldface); and 3) the coding sequence for the 5 C-terminal residues of TSV-PA (underlined). The product, amplified with primers En and EcR, was first subcloned into a pGEM vector (Promega). After digestion with *Bam*HI and *Eco*RI, the recovered TSV-PA open reading frame was ligated into the pET17b vector at *Bam*HI and *Eco*RI sites, to generate the expression plasmid, designated pET(tsvpa). The constructed plasmid was sequenced on both strands to ensure that the coding sequence of TSV-PA was correct.

Site-specific Mutagenesis—The construction of expression plasmids for TSV-PA variants was followed by overlap extension using polymerase chain reaction techniques, mainly as described by Ho *et al.* (15). Using pET(tsvpa)15 as the template, one fragment was amplified between primer Vn, in the sense direction, containing specific alterations in the nucleotide sequence and an antisense T_7 terminal primer (GCTAGTTATTGCTCAGCGG), located downstream of the TSV-PA coding sequence. Another fragment was amplified between the antisense primer VnR (reverse complementary to Vn) and a sense primer located in the T_7 promoter sequence (TAATACGACTCACTATAGGG). The resulting fragments were purified by gel electrophoresis on polyacrylamide gels and combined in a subsequent "fusion" reaction in which the overlapping ends annealed. Polymerase chain reaction amplification was then carried out between the T_7 promoter and terminal primers. The resulting 1-kilobase pair fragment was also purified by gel electrophoresis, digested by *Bam*HI and *Eco*RI, and ligated into the pET17b vector. The entire sequence encoding mutated TSV-PA was then verified by sequencing both DNA strands. The synthetic oligonucleotides used to generate the TSV-PA variants are listed in Table I.

Expression and Renaturation of Wild Type and TSV-PA Variants—The *E. coli* strain BL21(DE3) was transformed with plasmid of wild type, pET(tsvpa), or of TSV-PA variants. Cells were grown at 37 °C up to an absorbance of about 0.6 at 600 nm and then induced with 0.4 mM isopropyl-1-thio-β-D-galactopyranoside and cultivated for an additional period of 3 h at 37 °C. After cell lysing, inclusion bodies containing TSV-PA or mutated TSV-PA were recovered by centrifugation, washed three times with 50 mM Tris-HCl, pH 8.0, containing 2.5 mM EDTA, and then dissolved in 8 M urea in distilled water at room temperature for 30 min. The sample was dialyzed against 50 mM Tris-HCl, pH 8.0, 0.25 M NaCl, 2 mM EDTA at room temperature for 150 min. Bovine factor Xa was added at an enzyme:substrate ratio of 1:100, and digestion was conducted overnight at 37 °C. The protein was then fully denatured by dilution into 10 volumes of 8 M urea in 50 mM Tris-HCl, pH 8.0, 2 mM EDTA, containing 50 mM β-mercaptoethanol and incubated in the buffer for 120 min at room temperature. Refolding was started by diluting the sample 50 times in 50 mM Tris-HCl, pH 8.0, 2 mM EDTA. The refolding process was allowed to proceed at room temperature and was monitored by assaying the amidolytic activity of TSV-PA on chromogenic substrate S-2238. When the enzyme activity reached a plateau, after about 30–48 h, the refolding mixture was stored at 4 °C for subsequent purification. N-terminal sequence determinations of the recombinant protein were performed by Edman degradation with a 470A gas phase sequencer.

Purification of Recombinant Wild Type and Mutated TSV-PA—The purification of refolded wild type and mutated proteins was performed according to the last purification step used for natural TSV-PA from *T. stejnegeri* venom (1). The refolded protein was concentrated in an Amicon stirred cell concentrator under nitrogen pressure.

Measurement of Enzyme Concentration—Enzyme concentrations were determined by the Bio-Rad protein assay. To determine the molar concentration of the active site enzyme, wild type and mutated rTSV-PA were subjected to active site titration with 4-methylumbelliferyl *p*-guanidinobenzoate (16), using a Kontron spectrofluorimeter. Titrations were performed in 50 mM Tris-HCl (pH 8.0) containing 100 mM NaCl.

SDS-Polyacrylamide Gel Electrophoresis—SDS-PAGE was performed on a Phastsystem apparatus (Pharmacia) following the manufacturer's directions.

Immunochemical Analysis of rTSV-PA—Purified rTSV-PA was tested by enzyme-linked immunosorbent assay using rabbit polyclonal antibodies raised against natural TSV-PA. Competition experiments were performed as described by Choumet *et al.* (17). Briefly, various concentrations of natural or rTSV-PA were incubated for 12 h at 4 °C with a fixed dilution of anti-TSV-PA antibodies as deduced from preliminary enzyme-linked immunosorbent assay calibration. One hundred μl of each mixture were then transferred onto a microtitration plate previously coated with native TSV-PA and incubated for 1 h at 37 °C. Subsequent steps were performed as described above. The concentration of natural or rTSV-PA that gave half of the maximal response (IC_{50}) was determined.

Chromogenic Assays and Kinetic Analyses—The amidolytic activity of the enzymes was measured as described before (1). The kinetic parameters K_m and k_{cat} were determined by analysis of double-reciprocal plots of the initial velocity as a function of substrate concentration. The concentrations of the chromogenic substrates S-2238 and S-2251 varied from 0.3 mM to 0.01 mM in assays of all enzymes. The enzyme concentrations used were between 8 and 17 nM, except in the case of the TSV-PA variant D96aN/D97V/E98I, which was used at 55 nM. S-2302 and S-2444 substrate concentrations varied from 0.03 mM to 0.4 mM, and the final enzyme concentrations varied from 26 to 55 nM.

Plasminogen Activation Assays and Kinetic Analysis—The initial rate of plasminogen activation was measured with Lys-plasminogen as described previously (1). For kinetic analyses, Lys-plasminogen concentrations varied from 10 to 100 nM in the case of natural and recombinant wild type TSV-PA, the final concentration of TSV-PA being 10 nM. In the case of TSV-PA variants, Lys-plasminogen concentrations varied from 50 to 1000 nM, and the final concentration of the enzyme varied from 10 to 28 nM.

Topological Alignment and Modeling of TSV-PA—Modeling of the three-dimensional structure of TSV-PA (computations, visualization and analysis) was performed using the BIOPOLYMER and HOMOLOGY modules of the BIOSYM Technologies Inc. (San Diego, CA) software package.

The set of structurally conserved regions (SCRs) thus determined was based on the crystal structure of trigonal bovine pancreas trypsin (Protein Data Bank entry code 3PTN; Ref. 18). The choice for trypsin as the reference structure, rather than the functionally analogous u-PA (19) or t-PA (20) was justified by the fact that the B-chain of the C-terminal catalytic proteinase domain of u-PA contains several insertion fragments of considerable size, resulting in a total length of 248 residues compared with the 234 residues of TSV-PA. The length of trypsin (223 residues) is then closer to that of TSV-PA. Furthermore, five of the six disulfide bridges of TSV-PA are found in the same positions along the sequence in trypsin, as compared with four in the case of u-PA, one of the u-PA bridges linking the catalytic and kringle domains. The SCRs determined through structural alignment are in line with those of Greer (21), although they include minor modifications that take into consideration changes in the definition of certain segments due to an updated set of serine proteinases. As a first approximation, the loops were modeled as follows. When the loop length was the same, the backbone coordinates of TSV-PA were transferred from those of trypsin; in the case of one-residue insertions, the corresponding residue was inserted in the sequence, and the conformation of the new loop was energy-minimized. The conformations of the side chains of mutated residues were energy-minimized without any further refinement such as conformation search or rotamer assignment. Loop 142–151 of TSV-PA was obtained from the corresponding loop in u-PA, since the sequence homology was significantly higher than with trypsin. TSV-PA contains a C-terminal amino acid extension absent in trypsin and involved in the 91–245e cysteine bridge unique to TSV-PA. This fragment was model-built and optimized such as to ensure the formation of the corresponding disulfide bond. The stereochemical quality of the model was checked with the program PROCHECK (22). The numbering of the TSV-PA sequence is based on that of α-chymotrypsin.

RESULTS

Expression of TSV-PA in E. coli—After overexpression of TSV-PA in *E. coli*, a major protein of 30 kDa could be detected in whole cell extracts by SDS-PAGE. After denaturation, the

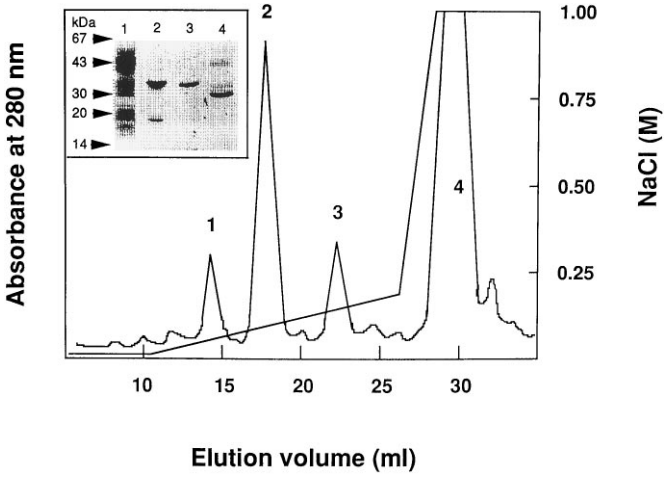

FIG. 1. **Purification of recombinant TSV-PA.** Refolded recombinant TSV-PA was concentrated and dialyzed against 20 mM Tris-HCl, pH 8.8, for 24 h. The sample was loaded on a fast performance liquid chromatography Mono-Q HR16/10 preparative column previously equilibrated with the same buffer. Elution was performed at a flow rate of 5.5 ml·min^{-1} with the NaCl gradient, as shown in the *figure*. The amidolytic activity and plasminogen activation activity was found in *peak 2*. *Inset*, SDS-PAGE (20% acrylamide). *Lane 1*, crude extract of induced cells; *lane 2*, isolated inclusion body; *lanes 3* and *4*, final purified recombinant TSV-PA. In *lanes 1–3*, SDS-PAGE was performed under reducing conditions (5% β-mercaptoethanol); in *lane 4*, it was performed under nonreducing conditions. Proteins were stained with Coomassie Brilliant Blue.

renaturation process yielded 20% of active enzyme. Active rTSV-PA was purified from misfolded protein and from contaminant bacterial proteins by chromatography in a Mono-Q anion exchange column (Fig. 1). The protein corresponding to peak 2 was able to hydrolyze chromogenic substrates and possessed plasminogen activation activity. This fraction corresponded indeed to rTSV-PA. The *inset* in Fig. 1 shows an SDS-PAGE analysis of the different fractions obtained by expression of TSV-PA in *E. coli*. Purified rTSV-PA reacted with polyclonal antibodies prepared against the natural enzyme. The IC_{50} determined through competition experiments was similar for recombinant and natural TSV-PA ($5{\cdot}10^{-7}$ M; data not shown).

Activity Assays and Kinetic Analyses of rTSV-PA—Titration of the active site in each molecule of natural and rTSV-PA gives a ratio of active site concentration to protein concentration of 0.97 ± 0.02 for both, indicating that rTSV-PA was fully active.

The activity of rTSV-PA on chromogenic substrates was characterized by the K_m and k_{cat} parameters obtained from Lineweaver-Burk plots for the synthetic substrates S-2238, S-2251, S-2302, and S-2444. Table II shows that the kinetic parameters of rTSV-PA with these substrates, when determined under the same conditions in parallel experiments, were not significantly different from those of natural TSV-PA. We also analyzed the kinetics of plasminogen activation by TSV-PA. TSV-PA activates Lys-plasminogen with a second order rate of 3.8 $\mu M^{-1}{\cdot}min^{-1}$ and with small Michaelis and catalytic constants (K_m = 53 nM, k_{cat} = 0.2 min^{-1}). We obtained the same result for rTSV-PA (Table II). K_m of TSV-PA on Lys-plasminogen activation is 35 times smaller than that of u-PA (K_m = 1.9 μM; Ref. 23). On the other hand, TSV-PA cleaves plasminogen with a k_{cat} 100 times and 50 times lower than that of u-PA and t-PA, respectively (24, 25).

Molecular Modeling—The topology-based sequence alignment between TSV-PA and trypsin is shown in Fig. 2. Fig. 3 shows a MOLSCRIPT representation (26) of the trypsin-like three-dimensional model of TSV-PA. As in all members of the family of serine proteinases (21), the topology of TSV-PA consists of two subdomains of antiparallel β-barrel structure (three strands in each subdomain) and a C-terminal helical segment. The spatial organization of the catalytic triad residues His^{57}, Asp^{102}, and Ser^{195} (7) at the active site cleft between the two subdomains is preserved in TSV-PA. The overall dimensions of TSV-PA are slightly larger than those of trypsin but smaller than those of u-PA. His^{217a} appears to reduce solvent accessibility to the gorge of the S1 specificity pocket. In the S2 pocket, a valine replaces the imidazole ring of His^{99} in u-PA. As a consequence, small hydrophobic residues usually found at the P2 position of known TSV-PA substrates can be accommodated. The C-terminal peptide of TSV-PA, contiguous to the large 234–243 helix, comprises a β-turn for residues 243–245a with Gly^{244} in the $i + 1$ position and an extended conformation for the Asp^{245b}–Pro^{245g} segment, which lies approximately perpendicular to the axis of the helix. This spatial arrangement will ensure the formation of the Cys^{91}/Cys^{245e} disulfide bridge characteristic of TSV-PA. All amide bonds are in *trans*.

Sequence comparison between TSV-PA and batroxobin identifies several regions where the two enzymes present a significant difference in amino acid sequence. Among those, the three segments, A, B, C (Table I), are exposed to the solvent in our three-dimensional model (Fig. 3). The loop ending at Val^{99} is smaller than that of u-PA and corresponds to region B of TSV-PA, made up of the charged peptide KKDDE 95–98, while the more hydrophobic SADTLA 95–98 segment lines the S2 pocket of u-PA. Region B is in close spatial proximity to the catalytic triad of the molecule, and the active site is thus slightly more accessible in TSV-PA than in u-PA, but less so than in trypsin. The S3 pocket is essentially composed of Gly^{216}, and the 95–99 loop does not extend to it as in u-PA. Upon imposing the canonical conformation of positions P5 to P1′ of the inhibitors complexed to trypsin, human α-thrombin, and u-PA (Protein Data Bank codes 1MCT, 1ABJ, and 1LMW, respectively) to the corresponding sequence of plasminogen, two features become apparent. First, the cyclic side chain of position P3 (Pro^{559}) points away from region B, and only the main chain-main chain hydrogen bond with Gly^{216} remains. Second, positions P6 (Lys^{556}) and P5 (Lys^{557}) of plasminogen, located next to the small disulfide loop containing the Arg^{561}–Val^{562} scissile bond (27) lie proximal to Asp^{97} of TSV-PA. Finally, the Cys^{128}–Cys^{232} disulfide bond in trypsin is replaced by a stacking interaction between Pro^{128} and Phe^{232} in TSV-PA, thus helping stabilize the long Pro^{128}–Val^{135} unstructured segment.

Other features of the three-dimensional model of TSV-PA common to the family of serine proteinases include the glycine at position 69, the characteristic CGG 42–44 sequence, and an internal salt bridge between the amino terminus and the side chain of the catalytic site residue Asp^{194}. Interestingly enough, in contrast to all trypsin-like serine proteinases that possess a glycine 193 at the S1 subsite, TSV-PA has a phenylalanine.

Mutagenesis of TSV-PA—To examine whether the three regions mentioned above might be implicated in the differential substrate specificities of TSV-PA, the variants constructed by replacing the corresponding amino acid residues by those of batroxobin (Table I), were expressed and purified as for the wild type enzyme. Under the same conditions, the renaturation yield of the variants varied from 7 to 20% and their elution from the Mono-Q column was slightly shifted according to their electric charge (results not shown).

For each TSV-PA variant the active site to protein concentration ratio per molecule, as determined by the Bio-Rad protein assay, was close to 1, as was the case for wild type rTSV-PA. Immunochemical analysis of TSV-PA variants by enzyme-

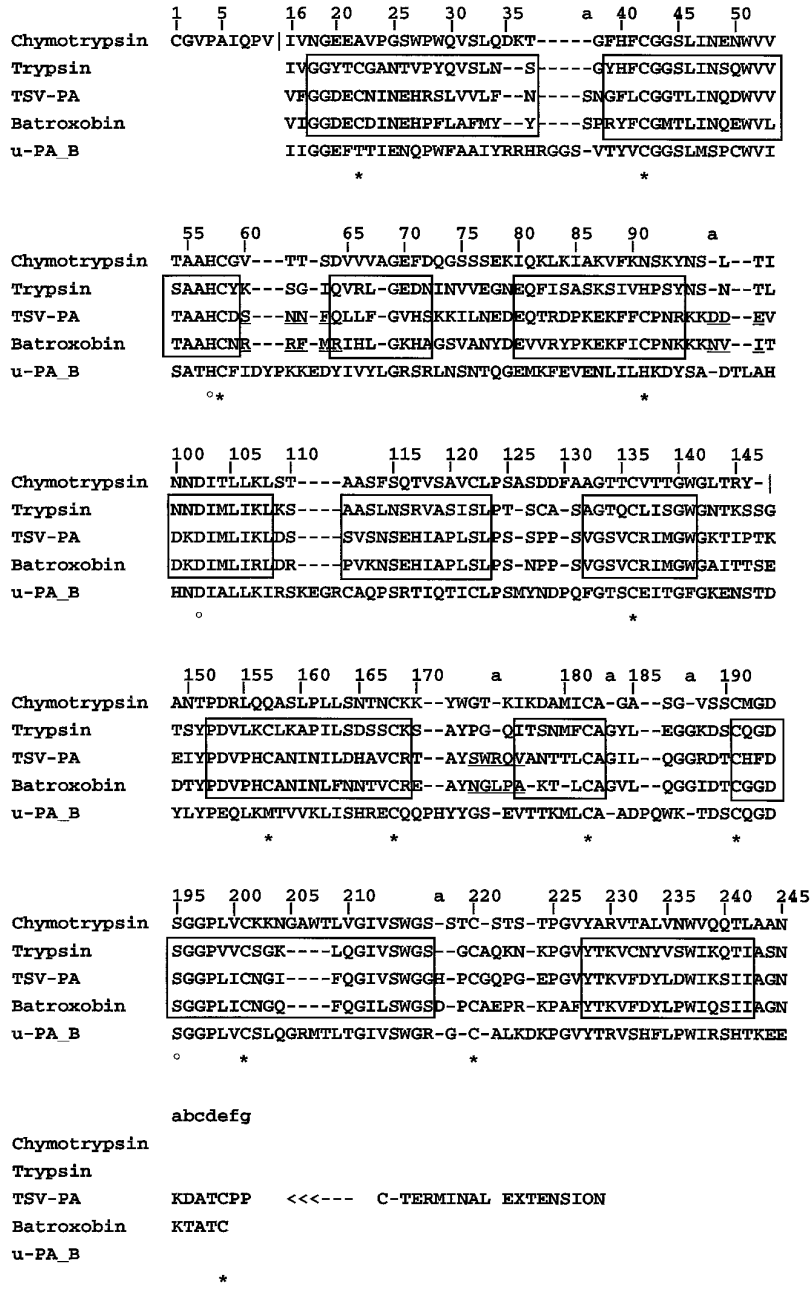

FIG. 2. **Nomenclature and structural alignment of the amino acid sequence of TSV-PA and trypsin.** The *first row* corresponds to the sequence of α-chymotrypsin. For the residues of TSV-PA and batroxobin, the α-chymotrypsin numbering system used is based upon the topological alignment with the structure of trypsin. Thus, the *second* and *third rows* show a structural alignment between trypsin and TSV-PA. In this nomenclature, residue Asn^{178}, for example, corresponds to Asn^{161} of Zhang *et al.* (1). The catalytic site residues are shown by *dots*, cysteines are shown by *asterisks*, and the SCRs are enclosed in *boxes*. The gaps introduced are the result of the optimal structural similarity obtained. The sequence of batroxobin, shown in the *fourth row*, is based upon a sequence alignment with TSV-PA. Regions probed by site-directed mutagenesis are *underlined*. These regions are S60R/N61R/N62F/F63M/Q64R, D96aN/D97V/E98I, and S173N/W174G/R174aL/Q175P/V176A. Insertions in TSV-PA with respect to α-chymotrypsin are denoted by *lowercase letters*, *e.g.* S37a. The catalytic domain of u-PA (29) is shown for comparison purposes.

linked immunosorbent assay showed that the IC_{50} values measured with each variant were similar to that of natural and rTSV-PA, suggesting that the mutations performed did not affect the epitope recognized by anti-TSV-PA antibodies and that the structural changes are due only to segment replacement and not to folding differences.

Activity of TSV-PA Variants on Chromogenic Substrates—All TSV-PA variants hydrolyzed S-2238, S-2444, and S-2251 but with significant quantitative differences (Table III). Detailed kinetic analyses revealed that replacement of residues 60–64, SNNFQ by RRFMR (mutant A), did not significantly modify the K_m and k_{cat} values of TSV-PA for these three substrates. Replacement of the distinctive electrically charged TSV-PA DDE 96a-98 region by the neutral sequence of batroxobin (NVI), mutant B, significantly increased the K_m value for S-2238 and S-2251 and abolished the activity on S-2444. We thus prepared the single point mutants B1 (D96aN), B2 (D97V), and B3 (E98I). As shown in Table III, the K_m values increased in some cases and decreased in others. The changes in k_{cat} displayed the same behavior too. For example, the k_{cat} value of D97V for S-2444 was about 8-fold lower than that of the wild type enzyme, whereas it was more than 3-fold higher for S-2238. In mutant C, replacement of the 173–176 peptide (SWRQV to NGLPA) modified slightly the k_{cat} value of the enzyme for these substrates, increasing it for S-2238 and S-2251 and decreasing it for S-2444 by about a factor of 2. The double mutant displayed the combined effects of individual replacements for S-2238, with slight increases in the K_m values of all three substrates, and 2–3-fold increases in the k_{cat} values of S-2238 and S-2251.

Activity of TSV-PA Variants on Plasminogen—Replacement of the 60–64 and 173–176 peptide (mutants A and C, and double mutant AC) did not abolish plasminogen activation by TSV-PA (Table III). However, the K_m for plasminogen was increased 4-fold over that of the wild type TSV-PA for mutant C and 22-fold for mutant AC, resulting in a significant change of the enzymatic activity of plasminogen. Interestingly enough, mutant B showed no detectable plasminogen activation activ-

ity, even when the sensitivity of the assay was increased 1000 times. Mutants B1, B2, and B3 retained some plasminogen activation activity but with significantly decreased affinity and rate constants. The most important effect was observed for B2, for which K_m increased by a factor of 25. For mutants B1, B2, and B3, the observed plasminogen activation changes widely (from 10- to 60-fold) with respect to the tripeptides (Table III).

Like TSV-PA, the variants did not show any direct fibrinogenolytic activity and did not clot a solution of purified fibrinogen, indicating the absence of thrombin-like activity (data not shown).

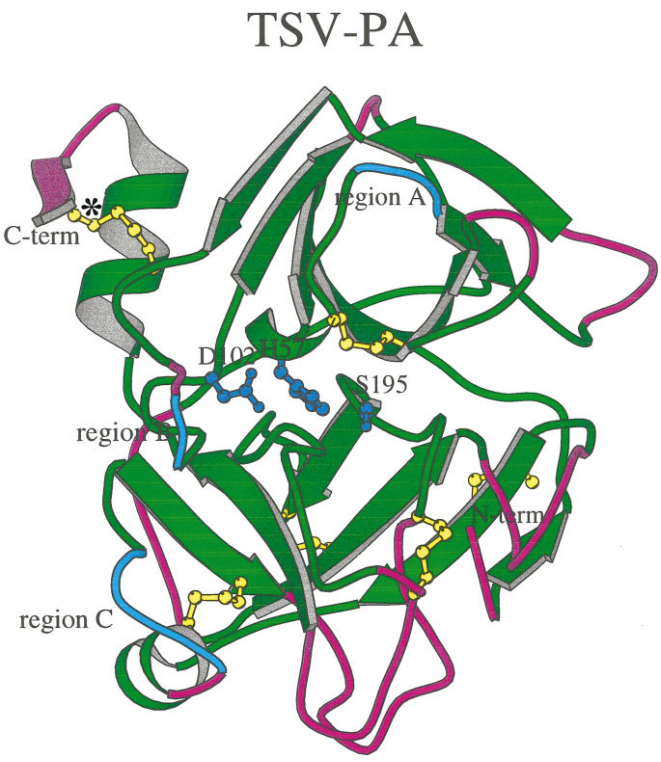

FIG. 3. **Diagram of the three-dimensional model of TSV-PA.** Shown is a MOLSCRIPT (26) representation of the main chain of TSV-PA showing the secondary structure elements, with the disulfide bridges in *yellow*, the catalytic triad His^{57}, Asp^{102}, and Ser^{195} in *blue*, the SCRs in *green*, and regions A, B, and C in *cyan*. The C-terminal extension characteristic of snake venom serine proteases is indicated, as well as TSV-PA's additional disulfide bridge (*). The SCRs in the three-dimensional model of TSV-PA were generated on the basis of the crystal structure of trigonal pancreas bovine trypsin (Protein Data Bank code 3PTN).

DISCUSSION

Studies of structure-function relationships and of potential thrombolytic activities *in vivo* require in general large amounts of protein difficult to obtain by purifying TSV-PA from its natural source; *T. stejnegeri* snakes are rather rare, and their venom is quite expensive. To overcome this obstacle, we prepared rTSV-PA by production in the efficient *E. coli* expression system. With 12 cysteines and six disulfide bridges, the successful expression of rTSV-PA relied on the isolation of the protein from inclusion bodies, followed by a denaturation-renaturation process in appropriate redox conditions to allow for the correct formation of disulfide bridges. The kinetic parameters of rTSV-PA with synthetic substrates and plasminogen were like those of natural TSV-PA and were not influenced by the absence of glycosylation. Anti-TSV-PA antibodies recognized the natural and the recombinant TSV-PA with comparable sensitivity.

Trypsin and the serine proteinases of snake venoms share a common structure and are believed to have evolved from a common ancestor (5). While the central region surrounding the catalytic triad is highly conserved structurally (28), the surfaces of snake venom serine proteinases may show considerable shape differences given the wide variations in loop sequence and length. The arrangement of disulfide bonds is identical to that of trypsin, except that the Cys^{128}–Cys^{232} bond of trypsin is replaced by one involving the C-terminal cysteine (4), *i.e.* the Cys^{91}–Cys^{245e} bond in TSV-PA. The functional significance of this modification, as well as that of the 6–7-residue insertion at the C terminus, is unknown.

As opposed to trypsin, which displays a broad substrate specificity, venom serine proteinases, whose primary structure is highly conserved (60–75% identity among members of the

TABLE I

Structure-function analysis of TSV-PA: site-directed mutagenesis

The TSV-PA variants were constructed by polymerase chain reaction techniques as described under "Experimental Procedures." Only the sense primers are listed here; the VnR primers were exactly reverse complementary.

TSV-PA variants	Oligonucleotides
A S60R/N61R/N62F/F63M/Q64R	CACTGCGACAGGAGATTTATGCGGTTGCTGTTT
C S173N/W174G/R174aL/Q175P/V176A	AACAGCTTATAATGGGCTGCCGGCGGCAAACACA
AC S60R/N61R/N62F/F63M/Q64R, S173N/W174G/R174aL/Q175P/V176A	CACTGCGACAGGAGATTTATGCGGTTGCTGTTT
	AACAGCTTATAATGGGCTGCCGGCGGCAAACACA
B D96aN/097V/E98I	AGGAAAAAGAATGTCATAGTGGACAA
B1 D96aN	AGGAAAAAGAATGACGAAGTGGACAA
B2 D97V	AGGAAAAAGGATGTCGAAGTGGACAA
B3 E98I	AGGAAAAAGGATGACATAGTGGACAA

TABLE II

Enzymatic activity: comparison of natural TSV-PA and recombinant TSV-PA

The methods used for kinetic analyses are described under "Experimental Procedures." The data represent the mean of three determinations, which differed by 5–15%.

Substrate	Natural TSV-PA			Recombinant TSV-PA		
	K_m	k_{cat}	k_{cat}/K_m	K_m	k_{cat}	k_{cat}/K_m
	μM	min^{-1}	$\mu m^{-1}\ min^{-1}$	μM	min^{-1}	$\mu m^{-1}\ min^{-1}$
H-D-Phe-Pip-Arg-*p*-NA[a] (S-2238)	16	746	46.6	18	833	46.3
H-D-Val-Leu-Lys-*p*-NA (S-2251)	370	339	0.92	405	340	0.85
H-D-Pro-Phe-Arg-*p*-NA (S-2302)	170	103	0.61	330	100	0.30
H-D-Glu-Gly-Arg-*p*-NA (S-2444)	2500	568	0.23	2000	500	0.25
Lys-plasminogen	0.053	0.2	3.8	0.050	0.2	4.0

[a] *p*-NA, para-nitroaniline.

TABLE III

Kinetic analysis of TSV-PA variants on chromogenic substrates and plasminogen

Kinetic analyses were carried out as described under "Experimental Procedures." The data represent the mean of three determinations, which differed by 5–15% for chromogenic substrate assays and 15–22% for plasminogen activation assays.

TSV-PA variant	S-2238 (H-D-Phe-Pip-Arg-*p*-NA)[a]			S-2251 (H-D-Val-Leu-Lys-*p*-NA)			S-2444 (H-D-Glu-Gly-Arg-*p*-NA)			Lys-plasminogen		
	K_m	k_{cat}	k_{cat}/K_m	K_m	k_{cat}	k_{cat}/K_m	K_m	k_{cat}	k_{cat}/K_m	K_m	k_{cat}	k_{cat}/K_m
	μM	min^{-1}	$\mu m^{-1}\ min^{-1}$	μM	min^{-1}	$\mu m^{-1}\ min^{-1}$	μM	min^{-1}	$\mu m^{-1}\ min^{-1}$	μM	min^{-1}	$\mu m^{-1}\ min^{-1}$
Recombinant	18	833	46	405	340	0.85	2000	500	0.25	0.050	0.2	4.0
A	20	735	37	560	440	0.79	1700	549	0.32	0.065	0.09	1.4
C	91	1520	17	360	625	1.7	2500	195	0.078	0.20	0.18	0.9
AC	63	1294	21	560	992	1.8	2900	357	0.12	1.11	0.13	0.12
B	105	744	7.1	5100	357	0.070	ND[b]	ND		ND	ND	
B1	67	1492	22	1000	750	0.75	690	253	0.37	0.62	0.08	0.13
B2	667	2850	4.3	2500	720	0.29	1400	65	0.046	1.25	0.04	0.032
B3	17	868	51	560	260	0.46	1000	123	0.12	0.77	0.06	0.078

[a] *p*-NA, para-nitroaniline.

[b] ND, no detectable enzymatic activity.

family), show very specific recognition for their particular substrates. This is especially so for TSV-PA, factor V activator, and batroxobin, which act, respectively on plasminogen, factor V, and fibrinogen but do not cleave other macromolecular substrates. Sequence alignment reveals that sequence differences among venom serine proteinases are clustered in several regions that can naturally be thought to contribute to their substrate specificity. The three-dimensional model of TSV-PA (Fig. 3) shows that peptides A, B, and C (Table I), whose sequences differ considerably between TSV-PA and batroxobin, are located on surface regions of TSV-PA. The 6-residue loop containing peptide B is made up almost entirely of charged side chains (KKDDEV) and, of the three peptides, it is the closest to the catalytic site. The data in this work show that the conversion of DDE 96a-98 of TSV-PA to NVI of batroxobin (peptide B) resulted in undetectable activity for plasminogen and in no fibrinogen clotting activity. Replacement of each of the negatively charged residues in the site indicated that D97V is the most critical one. This point mutation resulted in a 125-fold decrease of TSV-PA activity for plasminogen activation. A possible explanation of this effect is the spatial proximity of the DDE loop to the catalytic site. Once the substrate is appropriately placed on the site, this closeness leads to direct electrostatic interactions between Asp^{97} of TSV-PA and the residues vicinal to the scissile peptide bond of plasminogen (Lys^{556}-Lys^{557}). This is in agreement with the crystallographic structure determination of u-PA and t-PA, which shows that the 99-loop of t-PA contains three carbonyl groups directed toward the active site serving as anchoring parts for hydrogen bonds (20) and that a two-residue hydrophobic extension extends the same loop to form a lip to the binding cleft for u-PA (19). On the other hand, mutant B increased the K_m for the chromogenic substrates S-2238 and S-2251 but showed no activity for S-2444. These findings support the idea that replacement of residues in segment B affects tripeptide substrate cleavage and plasminogen differentially, the effect on plasminogen being much larger. Substitution of region A of TSV-PA, SNNFQ 60–64, by that of batroxobin (RRFMR) does not significantly modify the catalytic parameters of TSV-PA. This suggests, in fact, that this loop has little effect in general and is not critical to the plasminogen specificity of TSV-PA. In a similar vein, the experimental data indicate that the region corresponding to loop C, SWRQV 173–176 of TSV-PA, has a moderate effect on all substrates.

In general, the specificities of TSV-PA, t-PA, and u-PA for small chromogenic substrates are quite different (Chromogenix Catalogue, Sweden, and our own data). Yet, just like t-PA and u-PA, TSV-PA acts specifically on plasminogen and exerts no activity on other blood coagulation factors.

TSV-PA shows a high specificity for plasminogen and promises to be an interesting biochemical and pharmacological tool for investigating fibrinolysis *in vitro* and *in vivo*. Altogether, our results suggest that, in analogy to t-PA (8), the interaction of TSV-PA with macromolecular substrates such as plasminogen is of a complex nature and depends on secondary site binding. Finally, plasminogen activators seem to show no apparent correlation between their activity toward small substrates on one hand and plasminogen on the other. Comparative structural studies of t-PA, u-PA, and TSV-PA may help to further understand the nature of this discrimination for plasminogen.

Acknowledgments—We thank Dr. X. Cousin (Unité des Venins, Institut Pasteur, Paris) for helpful advice in conducting the molecular biology experiments, Dr J. d'Alayer (Laboratoire de Microséquence, Institut Pasteur, Paris) for performing the amino acid sequence analyses, Dr. U. K. Nowak (Oxford Center for Molecular Sciences, University of Oxford, UK) for making available the coordinates of u-PA prior to appearance in the Protein Data Bank, and Dr. S. Anderson (Unité des Venins, Institut Pasteur, Paris) for stylistic revision of the manuscript.

REFERENCES

1. Zhang, Y., Wisner, A., Xiong, Y., and Bon, C. (1995) *J. Biol. Chem.* **270,** 10246–10255
2. Robbins, K. C., Summaria, L., Hsieh, B., and Shah, R. J. (1967) *J. Biol. Chem.* **242,** 2333–2342
3. Forsgren, M., Raden, B., Israelsson, M., Larsson, K., and Hedden, L.-O. (1987) *FEBS Lett.* **213,** 254–260
4. Nikai, T., Ohara, A., Komori, Y., Fox, J. W., and Sugihara, H. (1995) *Arch. Biochem. Biophys.* **318,** 89–96
5. Itoh, N., Tanaka, N., Funakoshi, I., Kawasaki, T., Mihashi, S., and Yamashina, I. (1988) *J. Biol. Chem.* **263,** 7628–7631
6. Neurath, H. (1985) *Fed. Proc.* **44,** 2907–2913
7. Perona, J., and Craik, C. S. (1995) *Protein Sci.* **4,** 337–360
8. Ding, L., Coombs, G. S., Strandberg, L., Navre, M., Corey, D. R., and Madison, E. L. (1995) *Proc. Natl. Acad. Sci. U. S. A.* **92,** 7627–7631
9. Tokunaga, F., Nagasawa, K., Tamura, S., Miyata, T., Iwanaga, S., and Kisiel, W. (1988) *J. Biol. Chem.* **263,** 17471–17481
10. Itoh, N., Tanaka, N., Mihashi, S., and Yamashina, I. (1987) *J. Biol. Chem.* **262,** 3132–3135
11. McMullen, B. A., Fujikawa, K., and Kisiel, W. (1989) *Biochemistry* **28,** 674–679
12. Hessel, B., and Blomback, M. (1971) *FEBS Lett.* **18,** 318–320
13. Maeda, M., Satoh, S., Suzuki, S., Niwa, M., Ioth, N., and Yamashina, I. (1991) *J. Biochem.* (*Tokyo*) **109,** 632–637
14. Wallen, P., and Wiman, B. (1972) *Biochim. Biophys. Acta* **257,** 122–134
15. Ho, S. N., Hunt, H. D., Horton, R. M., Pullen, J. K., and Pease, L. R. (1989) *Gene* (*Amst.*) **77,** 51–59
16. Jameson, G. W., Roberts, D. V., Adams, R. W., Kyle, S. A., and Elmore, D. T. (1973) *Biochem. J.* **131,** 107–117
17. Choumet, V., Jiang, M. S., Radvanyi, F., Ownby, C., and Bon, C. (1989) *FEBS Lett.* **244,** 167–173
18. Bernstein, F. C., Koetzle, T. F., Williams, G. J. B., Meyer, E. F., Brice, M. D., Rodgers, J. R., Kennard, O., Shimanouchi, T. C., and Tasumi, M. (1977) *J. Mol. Biol.* **112,** 535–542
19. Spraggon, G., Phillips, C., Nowak, U. K., Ponting, C. P., Saunders, D., Dobson, C. M., Stuart, D. I., and Jones, E. Y. (1995) *Structure* **3,** 681–691
20. Lamba, D., Bauer, M., Huber, R., Fisher, S., Rudolph, R., Kohnert, U., and Bode, W. (1996) *J. Mol. Biol.* **258,** 117–135
21. Greer, J. (1990) *Proteins Struct. Funct. Genet.* **7,** 317–334
22. Laskowski, R. J., MacArthur, M. W., Moss, D. S., and Thornton, J. M. (1993)

J. Appl. Crystallogr. **26,** 283–291
23. Wohl, R. C., Summaria, L., and Robbins, K. C. (1980) *J. Biol. Chem.* **255,** 2005–2013
24. Hoylaerts, M., Rijken, D. C., Lijnen, H. R., and Collen, D. (1982) *J. Biol. Chem.* **257,** 2912–2919
25. Madison, E. L., Coombs, G. S., and Corey, D. R. (1995) *J. Biol. Chem.* **270,** 7558–7562
26. Kraulis, P. J. (1991) *J. Appl. Crystallogr.* **24,** 946–950
27. Pennica, D., Holmes, W. E., Kohr, W. J., Harkins, R. N., Vehar, G. A., Ward, C. A., Bennett, W. F., Yelverton, E., Seeburg, P. H., Heyneker, H. L., Goeddel, D. V., and Collen, D. (1983) *Nature* **301,** 214–221
28. Neurath, H. (1984) *Science* **224,** 350–357
29. Steffens, G. J., Gunzler, W. A., Otting, F., Frankus, E., and Flohé, L. (1982) *Hoppler Seyler's Z. Physiol. Chem.* **363,** 1043–1058